

SIMULATION OF DETAILED CHEMISTRY IN A TURBULENT COMBUSTOR FLOW

H. C. MAGEL, U. SCHNELL AND K. R. G. HEIN

*Institute for Process Engineering and Power Plant Technology
University of Stuttgart
Pfaffenwaldring 23, D-70550 Stuttgart, Germany*

This paper describes the inclusion of detailed chemical reaction mechanisms in the framework of a turbulent flame simulation. Calculations are based on a finite-volume solution procedure including submodels for turbulent flow, radiative heat transfer, combustion of fuel, and pollutant formation. The interaction of chemical reactions and turbulence is modeled using the eddy dissipation concept (EDC), which has been extended to include detailed chemical reaction mechanisms.

For the oxidation of methane, a detailed C_1/C_2 mechanism is compared with a skeletal mechanism, which is also used to calculate the formation of nitrogen oxide. The basic idea of incorporating the reaction mechanism into the EDC is described. The numerical effort of the resulting coupled partial differential equation system involved investigations of adequate reduction methods.

The proposed model is applied to a 400-kW turbulent diffusion methane flame in a cylindrical furnace of which experimental results are available for a detailed evaluation of the proposed method. Predictions are performed with full and skeletal mechanisms. The measured trends in temperature and species concentrations of CH_4 , O_2 , CO , CO_2 , and NO are reproduced adequately by the predicted profiles.

Steady-state conditions have been introduced for many of the radical concentrations. In this way, the numerical effort can be lowered considerably without affecting the results compared to calculations without steady-state conditions.

Postprocessor calculation of the NO chemistry shows some differences compared with the coupled solution. However, considering the uncertainties and simplifications included in a turbulent flame calculation, the postprocessor calculation shows reasonable agreement. Investigations on the mechanisms of NO formation reveal that the calculated thermal NO cannot account for the experimentally observed NO , and prompt NO makes a significant contribution to the NO emission of this flame.

Introduction

Prediction of flames in furnaces is an important tool for the development of optimized combustion methods. Since chemical kinetics have a major influence on formation and destruction of pollutants and intermediate species such as carbon monoxide, a more detailed modeling of turbulent combustion for advanced combustion systems equipped with air or fuel staging is required. Turbulent flame predictions may be improved significantly if the combustion model can account for phenomena such as ignition and extinction [1] and NO_x formation. The best way to account for chemical kinetic effects is to apply a detailed reaction mechanism. In the following, we will outline a combustion model that is able to handle a detailed reaction mechanism based on the eddy dissipation concept (EDC). The model is applied to a turbulent diffusion methane flame in a furnace of which experimental results are available for a detailed evaluation of the proposed method.

Mathematical Models

A prediction code for turbulent reacting flows includes submodels describing flow field, combustion, and heat transfer by radiation. In their entirety, the different submodels form a system of strongly coupled partial differential equations. Each of these equations can be written in the form of a general transport equation:

$$\frac{\partial}{\partial x} (\rho u \Phi) = \frac{\partial}{\partial x} \left(\Gamma \frac{\partial \Phi}{\partial x} \right) + S_\Phi \quad (1)$$

where ρ , u , x , S_Φ , and Γ are density, velocity, coordinates, source term, and diffusion coefficient, respectively. This equation describes the local change of the Favre-averaged variable Φ caused by convection, diffusion, and production under steady-state conditions. Depending on Φ , Eq. (1) represents mass, momentum, species, or energy conservation.

Fluid Mechanics and Thermal Radiation

The basic equations of numerical fluid mechanics are well described in numerous preceding papers [2] and only the newly incorporated features are related here. The Navier–Stokes equations are solved for the primitive variables with a standard k,ε -turbulence closure. A transport equation, Eq. (1), is solved for the mean mass fraction of each balanced species. The mass density is determined by the ideal gas equation of state. Thermal radiation is modeled using the discrete transfer method proposed by Lockwood and Shah [3]. The absorption coefficient of the gas mixture is assumed to have a constant value of 0.5/m.

Turbulent Combustion

Chemical reactions are only functions of the local state specified by density, species concentrations, and enthalpy and can be described properly with a detailed reaction mechanism. Because of the statistical nature of these variables in turbulent combustion and the nonlinearity of chemical reaction rates, however, the current computational limits prohibit a complete description of chemistry and turbulent flow. Therefore, a turbulent combustion model based on simplifications in describing the turbulence behavior and the chemical reaction mechanisms is necessary to calculate the mean reaction rates.

Chemical reaction kinetics have been included explicitly in a number of turbulent flame studies in conjunction with a full H_2 mechanism and presumed-shape joint PDFs [4] or with reduced chemistry and Monte Carlo calculations of the joint PDF [5,6].

In this study, the EDC is used to model the influence of turbulence on chemical reactions. With the EDC, it is possible to include a detailed reaction mechanism in turbulent flame calculations. The presented EDC combined with chemical kinetics is a general concept that allows inclusion of radiation, fuel generated by particles, and the simulation of furnaces with multiple inlets with different fuel composition.

Numerical Solution

A conventional finite-volume method is used to solve the system of partial differential equations. For the nonstaggered grid arrangement a special procedure, known as the pressure-weighted interpolation method (PWIM), is needed to calculate the convective fluxes at volume faces. To reduce numerical diffusion, the monotonized linear-upwind (MLU) scheme is used for the calculation of the convective fluxes. The equations are solved using a Gauss–Seidel algorithm. To accelerate the convergence rate, the pressure-correction equation is solved using the

strongly implicit procedure. The SIMPLEC algorithm is chosen for the treatment of velocity–pressure coupling. Further details of the numerical solution procedure have been published previously by Schneider et al. [7].

Chemical Reaction Mechanisms for Methane

The oxidation of methane is quite well understood and various detailed reaction mechanisms are reported in literature. They can be divided into full mechanisms, skeletal mechanisms, and reduced mechanisms. The various mechanisms differ with respect to the considered species and reactions. Peeters [9] shows the effects of some mechanisms on laminar flame speed, maximum temperature, and CO concentration. However, considering the uncertainties and simplifications included in a turbulent flame calculation, the various mechanisms agree reasonably well. A detailed description of the treatment of elementary reaction systems can be found in Kee [8]. The two following mechanisms are investigated:

The Full C_1/C_2 Mechanism of Warnatz and Maas

The most comprehensive reaction mechanism used in this work is the full C_1/C_2 mechanism, taken from Warnatz and Maas [10], by allowing C_1 and C_2 species only. This mechanism includes about 100 elementary reactions and considers the following 27 species: CH_4 , O_2 , CO_2 , H_2O , CO , H_2 , H , O , OH , N_2 , HCO , CH_2O , H_2O_2 , HO_2 , CH_3 , CH_2 , CH , C_2H_6 , C_2H_5 , C_2H_4 , C_2H_3 , C_2H_2 , C_2H , $HCCO$, CH_2CO , CH_3CO , CH_3HCO . This full mechanism is believed to capture the most important reactions with sufficient accuracy.

The Skeletal Mechanism of Glarborg et al.

The skeletal mechanism determined and reported by Glarborg et al. [11] is derived from the full mechanism published by Miller and Bowman [12] but neglects certain species and reactions. This subset is valid only for certain flame conditions. It includes about 50 elementary reactions and considers the following species for the methane chemistry: CH_4 , O_2 , CO_2 , H_2O , CO , H_2 , H , O , OH , N_2 , HCO , CH_2O , CH_2OH , HO_2 , CH_3 , CH_2 , $CH_2(S)$, CH , C . The nitrogen chemistry accounts for the species HCN , NO , N_2O , N , NH , CN , NCO using 27 reactions.

The most important simplification of the skeletal mechanism is that the C_2 -hydrocarbon chemistry has been excluded. According to Glarborg, this mechanism should be able to describe the chemistry from lean to moderate fuel-rich conditions ($\Phi < 1.4$) at reasonable computational costs. Special emphasis has been put on the formation and destruction of hydrocarbon radicals because of their importance in

nitrogen chemistry. The nitrogen chemistry includes thermal NO and prompt NO formation, as well as the NO-to-HCN recycle reactions and a conversion of HCN to NO and \dot{N}_2 . The reactions with NH_3 and NH_2 , however, are neglected. The mechanism has been developed to describe methane combustion in perfectly stirred reactors and is therefore of special interest here, because the concept employed to couple chemistry and turbulence is based on perfectly stirred reactor calculations.

Eddy Dissipation Concept (EDC)

As proposed by Magnussen [13,14], the EDC is a general concept for treating the interaction between turbulence and chemistry in flames. The method is based on a detailed description of the dissipation of turbulent eddies. In the EDC, the total space is subdivided into a reaction space called the *fine structures* and the *surrounding fluid*. All reactions of the gas-phase components are assumed to take place within this reaction space that represents the smallest turbulence scales where all turbulent energy is dissipated into heat. So all reactions in the surrounding fluid are neglected. This assumption is the main simplification and has to prove its validity in practical applications.

Following Magnussen [13], the flow rate M^* per unit time can be derived from a consideration of the decay rate of turbulence

$$M^* = 2.43 \left(\frac{\varepsilon}{\nu} \right)^{0.5} \quad (2)$$

with the dissipation of turbulent kinetic energy ε and the kinematic viscosity ν . The original formula for the mass fraction γ^* occupied by the fine structures has shown good results in swirling flame calculations [15]:

$$\gamma^* = [2.13 (\nu\varepsilon/k^2)^{0.25}]^3 \quad (3)$$

with the turbulent kinetic energy k . Recently, it has been argued [16,17] that γ^* should be modeled as

$$\gamma^* = [2.13(\nu\varepsilon/k^2)^{0.25}]^2 \quad (4)$$

In this work, Eq. (4) is used because it has shown better agreement with experimental data. The fraction of the fine structures is larger using Eq. (4) rather than Eq. (3). This is more realistic in situations with low turbulence level and slow chemistry. For now, it is unavoidable to employ some empirical description of turbulence decay according to the prevailing turbulent flow situation. However, the choice of the formula does not affect the general concept of treating the fine structures as a well-stirred reactor.

The mass flow rate M per unit mass of fluid (and time) is related to the mass flow rate per unit mass

of the fine structures M^* and the mass fraction of fine structure γ^* through

$$M = M^*\gamma^* \quad (5)$$

The mean net mass transfer rate of a species i between the fine structures and the surrounding fluid can be expressed as

$$R_i = \frac{\bar{\rho}M\chi}{1 - \gamma^*\chi} (m_i - m_i^*) \quad (6)$$

where $\bar{\rho}$ is the local mean density of the gas, m_i is the local mean value of the mass fraction of species i , and m_i^* is its value in the fine structures. The correction factor χ designates the fraction of the fine structures that is heated sufficiently and may react. χ accounts for finite-rate chemistry effects when the fast chemistry assumption is used. Since chemical kinetics are included in the present work, $\chi = 1$.

Well-Stirred Reactor

By treating the reacting fine structures locally as a well-stirred reactor that transfers mass and energy only to the surrounding fluid, every chemical kinetic mechanism can be linked with the EDC combustion model. The reaction rates of all species are calculated on a mass and enthalpy balance for the fine structure reactor. Denoting quantities in the fine structures with an asterisk, the chemical reactions and the mass transport can be described by the following algebraic equations for species conservation and total enthalpy \dot{h} :

$$\frac{M^*}{1 - \gamma^*\chi} (m_i^* - m_i) = \frac{\omega_i^* W_i}{\rho^*} \quad (i = 1, \dots, I) \quad (7)$$

$$\frac{M^*}{1 - \gamma^*\chi} \sum_{i=1}^I (m_i^* h_i^* - m_i h_i) = \frac{q^*}{\rho^*} \quad (8)$$

q^* is the net energy rate per volume that is transferred between the fine structures and the surroundings by other mechanisms such as radiation, ω_i^* are the chemical reaction rates, and W_i is the molecular weight.

From Eqs. (7) and (8), it is possible to calculate the mass fractions m_i^* and temperature T^* in the fine structures as a function of the known quantities T and m_i (mean temperature and mean mass fractions, respectively). The mean reaction rates of all species can then be calculated by using either the mass transfer rate expressed by Eq. (6) or the chemical reaction rate ω_i^* inside the fine structures. One should keep in mind that the reactions take place only within a fraction of the total space defined by Eq. (4). Since the chemical reaction rates ω_i^* in the fine structures in general are functions of all the mass fractions and the temperature, a set of nonlinear, coupled, algebraic equations must be solved.

Numerical Solution

The solution of the perfectly stirred reactor (PSR) equations, Eqs. (7) and (8), must be obtained by an *inner* iteration procedure, which is embedded in the CFD-iteration procedure of the general transport equations, see Eq. (1). This means that for each CFD iteration, it is necessary to calculate at least once the Jacobian matrix of the PSR equation system in each control volume. This is performed with a modified version of the PSR code from the CHEMKIN library [18]. A good initial estimate is required to prevent numerical problems. The calculations with detailed chemistry are always started from a converged solution obtained with a global two-step chemistry [15].

A turbulent flame calculation with detailed chemistry needs a large amount of CPU time consumed by the solution of a nonlinear equation system to determine the source terms of the species. In addition, many CFD iterations are necessary to converge all species concentrations, particularly the radical concentrations. A common method to reduce the complexity of the system is to decouple the nitrogen chemistry from the fuel oxidation process and solve it in a postprocessing step. Another reduction technique is to introduce steady-state conditions for radicals.

Steady-State Condition for Radicals

Steady-state assumptions for radicals inside the fine structure reactor reduce the number of mass fractions for which a transport equation must be solved. This way, the number of necessary CFD iterations can be lowered considerably because the radical concentrations need many CFD iterations to converge. However, the solution of the nonlinear PSR equation system may cause even more numerical difficulties.

Steady-state conditions can be included in the PSR equation system with ease. The species are split into two groups. The *main species* are independent reactive species for which a transport equation (see Eq. [1]) is solved. For the *steady-state species*, chemical production and consumption inside the reactor are assumed to be equal. This means that all the reactions of the employed mechanism are possible reaction paths inside the reactor but the steady-state species are not affected by the reactor inlet conditions (the surrounding fluid) and therefore no transport equations need to be solved.

A steady-state condition for a certain species i is established by setting the reactor inlet concentration equal to the concentration inside the reactor:

$$m_i = m_i^* \quad (i: \text{steady-state species}) \quad (9)$$

This omits the transport term for steady-state species and leads to the PSR equation system consisting

of Eq. (7) for $i \equiv$ main species, the following Eq. (10) for $i \equiv$ steady-state species

$$0 = \frac{\omega_i^* W_i}{\rho^*} \quad (10)$$

and Eq. (8) for enthalpy. This method calculates steady-state conditions accounting for all reactions of the mechanism without any analytical mathematical work. It is therefore applicable to every reaction mechanism, and species and reactions can be added and subtracted easily.

The skeletal mechanism of Glarborg et al. [11] is used to test the proposed reduction technique. Treating CH_4 , O_2 , CO_2 , H_2O , CO , H_2 , H , O , OH , and N_2 as main species and applying steady-state assumptions for all the other species has proved quite satisfactory for the investigated turbulent combustor flow. Compared to calculations without steady-state assumptions, no significant influence on the calculated results is found and a proper solution of the PSR equation system is obtained. The numerical effort using the proposed method is only slightly higher compared to the reduced four-step mechanism proposed by Glarborg [11] that still requires the calculation of all reaction rates of the skeletal mechanism.

Turbulent Flame Calculation

Results of a turbulent diffusion flame in a cylindrical furnace with a thermal input of 400 kW are presented. A full description of this furnace and the experimental conditions can be found in Ref. 19. Fuel and air are fed through two co-axial pipes with diameters of 60 and 100 mm. The diameter and length of the combustion chamber are 0.5 and 1.7 m, respectively. The composition of the natural gas is approximately 90% methane and 10% nitrogen.

Although the overall fuel-to-air ratio is only moderately fuel rich ($\Phi = 1.04$), the local ratio, calculated from the sum of the remaining combustibles CH_4 , CO , and H_2 , can be much higher (Fig. 1). This ratio defines the inlet condition for the PSR calculations and is important when choosing the chemical reaction mechanism. The chemical reactions are quite slow in the mixing region between the two jets, leading to a slow temperature rise during the consumption of methane. These phenomena are reflected in the axial profiles of temperature, CH_4 , and CO_2 data (Fig. 2) and the radial profiles of CH_4 and O_2 data (Fig. 3), which are reproduced adequately by the predicted profiles using the full C_1/C_2 mechanism of Warnatz and Maas without any steady-state assumption. For the radial profiles, one must keep in mind that there is a steep gradient near the axis and in this region the profiles are very sensitive to even small shifts in the axial distance.

A computational grid with 65 nodes in axial and

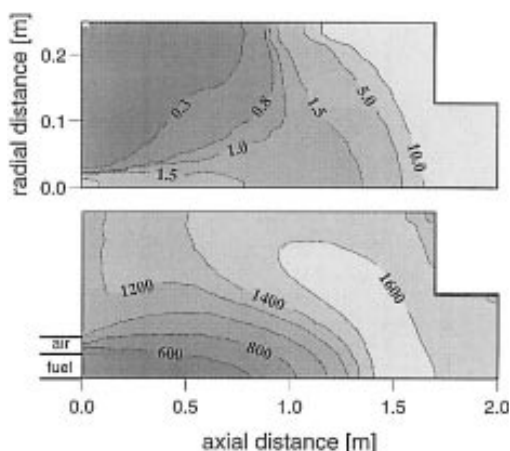


FIG. 1. Calculated temperature distribution in Kelvin (below) and local fuel/air ratio (above).

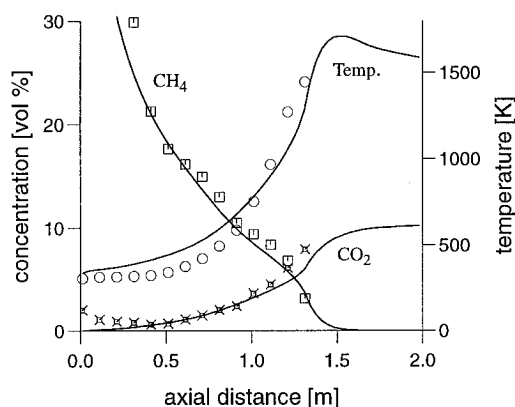


FIG. 2. Temperature and concentration of CH_4 and CO_2 along the flame axis using a C_1/C_2 mechanism. Symbols: data; lines: predictions.

30 nodes in radial direction was used. Calculations performed with a refined grid (130×70 nodes) gave almost identical results; therefore, grid independence is assumed.

Importance of the C_2 Reaction Chain

The C_2 reaction path is the dominant path in the cold ignition zone of the flame up to an axial distance of about 1.3 m (Fig. 4). In this region, however, the total reaction progress is very slow so that the C_2 chain does not have a decisive impact on the overall result, as shown later.

Results Obtained with Different Reaction Mechanisms

A comparison of the full C_1/C_2 mechanism of Warnatz and Maas and the skeletal C_1 mechanism of

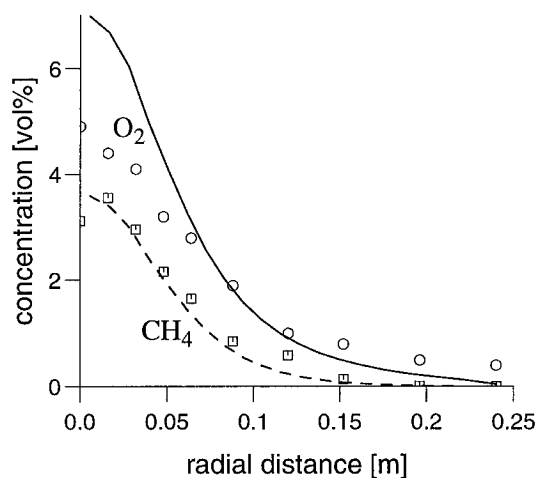


FIG. 3. Radial profile of CH_4 and O_2 concentration at an axial distance of 1.31 m. Circles: O_2 data; boxes: CH_4 data; solid line: O_2 prediction; dashed line: CH_4 prediction.

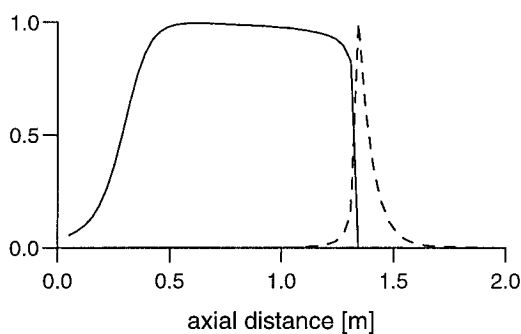


FIG. 4. Fraction of CH_3 reacting via C_2 chain (solid line) and total normalized consumption rate of CH_3 (dashed line) along the flame axis.

Glarborg et al. is shown in Fig. 5. Neglect of the C_2 chain causes some differences in ignition and intermediate species such as CO. However, the mechanisms do not differ much in predicting the general methane combustion progress. The profiles calculated with the skeletal mechanism using the steady-state assumptions described previously do not show any visible difference from the profiles without reduction and are therefore not shown in Fig. 5.

Predictions of Nitrogen Oxide

The skeletal mechanism of Glarborg et al. [11] is used to calculate nitrogen oxide. The predicted axial profile agrees well with the available measurements (see Fig. 6). Unfortunately, no data are available beyond an axial distance of 1.31 m, which would allow a complete validation. The radial profile at an axial

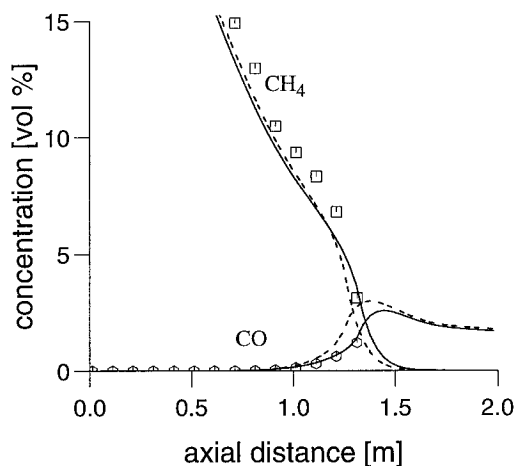


FIG. 5. Comparison of CH_4 and CO concentrations. Symbols: data; solid lines: predictions using a full C_1/C_2 mechanism; dashed lines: predictions using a skeletal C_1 mechanism.

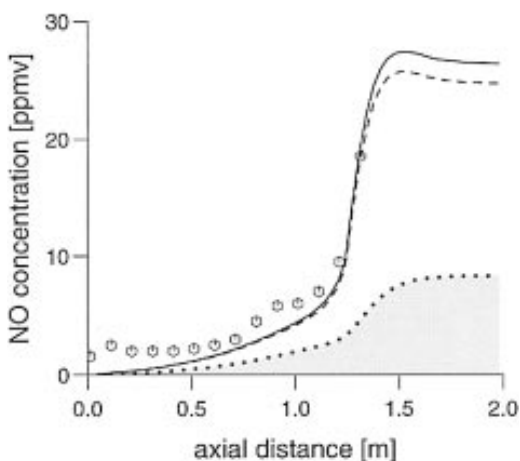


FIG. 6. Axial profiles of NO concentration. Symbols: data; solid line: coupled prediction; dashed line: postprocessor prediction; dotted line: thermal NO (coupled prediction).

distance of 1.31 m (Fig. 7) shows that the calculated NO concentration is a little underpredicted. Following an idea of Miller and Bowman [12], the fraction of thermal NO is investigated by deleting the prompt NO initiation reactions. The calculated thermal NO cannot account for the experimentally observed NO and is only about one-third of the total NO. This shows that prompt NO makes a significant contribution to the NO emission in the prediction of this flame.

The calculation of the nitrogen chemistry as a

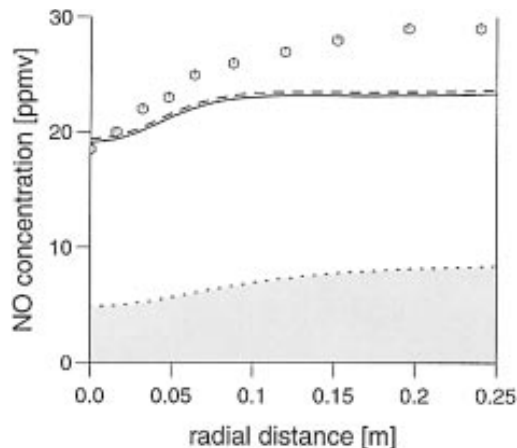


FIG. 7. Radial profiles of NO concentration at an axial distance of 1.31 m. Symbols: data; solid line: coupled prediction; dashed line: postprocessor prediction; dotted line: thermal NO (coupled prediction).

postprocessor differs slightly from the coupled solution. But, considering the uncertainties and simplifications included in a turbulent flame calculation, the postprocessor calculation shows reasonable agreement and significantly reduces the computational effort. A further reduction by treating only HCN, NO, and N_2 as main species and applying steady-state conditions to N_2O , N, NH, CN, and NCO brings about identical NO results, even if the steady-state assumptions described are used to calculate methane combustion. This demonstrates again the potential of reducing detailed chemistry in turbulent flame calculations without affecting the results.

Influence of Fuel Composition

Because in many technical flames the fuel composition may not be constant or known exactly, the sensitivity of calculations to the fuel composition is investigated. Therefore, 20% of the CH_4 mass flow is replaced with C_2H_6 and H_2 such that the elemental composition of C, H, and N does not change.

The O_2 concentrations of both calculations (Fig. 8) show that the ignition of the fuel mixture is somewhat faster. Obviously, differences exist as for the substitute fuel components (e.g., for H_2 , which is now fed as fuel and initially present in the flame). The discrepancies in the predicted H_2 profiles vanish after the flame zone. A certain influence is found with most of the radical concentrations, such as OH, which has an impact on the calculation of NO.

Conclusions

A combustion model capable of representing detailed chemical reaction mechanism in the

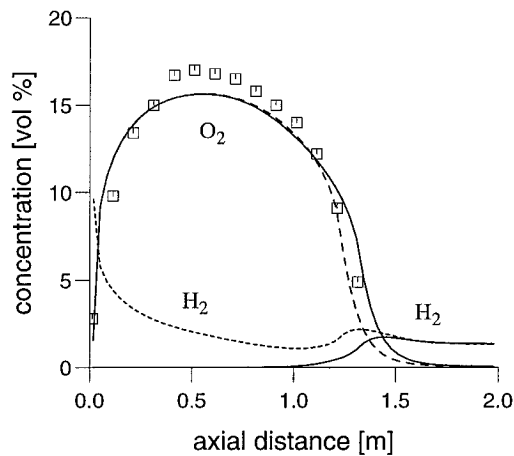


FIG. 8. Influence of fuel composition on predicted O₂ and H₂ concentrations. Symbols: data of O₂; solid lines: prediction with pure CH₄; dashed lines: prediction with fuel mixture (see text).

framework of a turbulent combustor flow simulation based on an eddy dissipation concept has been investigated. From the simulation of a 400-kW turbulent diffusion flame in a cylindrical furnace, the following main results have been obtained:

1. Predictions with full and skeletal reaction mechanisms of Warnatz and Maas [10] and Glarborg et al. [11] give good agreement with measured temperature and species concentration data. Because of the importance of the C₂ reaction path in the cold ignition zone of the flame, slightly different results are obtained for the CO concentration in particular.
2. The NO concentration profiles predicted with Glarborg's nitrogen chemistry agree well with the available data. Prompt NO was found to make a significant contribution to the NO emission of this flame.
3. Using the EDC, it is possible to apply steady-state conditions inside the fine structure reactor to many intermediate species without affecting the results.

REFERENCES

1. Gran, I. R., Melaaen, M. C., and Magnussen, B. F., *Twenty-Fifth Symposium (International) on Combustion*, The Combustion Institute, Pittsburgh, 1994, pp. 1283-1291.
2. Schnell, U., Schneider, R., Magel, H. C., Risio, B., Lepper, J., and Hein, K. R. G., Third International

- Conference on Combustion Technologies for a Clean Environment, Lisbon, 1995.
3. Lockwood, F. C. and Shah N. G., *Eighteenth Symposium (International) on Combustion*, The Combustion Institute, Pittsburgh, 1981, pp. 1405-1414.
4. Bockhorn, H., "Zur Struktur Turbulenter Diffusionsflammen," Habilitation Thesis, University of Darmstadt, 1989.
5. Pope, S. B., *Prog. Energy Combust. Sci.* 11:119-192 (1985).
6. Nau, M., Wölfert, W., Maas, U., and Warnatz, J., *Tenth Symposium on Turbulent Shear Flows* Vol. 2, 1995, pp. 19.25-19.30.
7. Schneider, R., Risio, B., Schnell, U., and Hein, K. R. G., Third International Symposium on Coal Combustion, Beijing, 1995.
8. Kee, R. J., Rupley, F. M., and Miller, J. A., "CHEMKIN-II: A Fortran Chemical Kinetics Package for the Analysis of Gas-Phase Chemical Kinetics," Sandia National Laboratories Technical report SAND89-8009, 1989.
9. Peeters, T., "Numerical Modeling of Turbulent Natural-Gas Diffusion Flames," Ph.D. Thesis, University of Delft, 1995.
10. Warnatz, J. and Maas, U., *Technische Verbrennung*, Springer Verlag, New York, 1993, pp. 101-104.
11. Glarborg, P., Lilleheie, N. I., Bygstol, S., Magnussen, B. F., Kilpinen, P., and Hupa, M., *Twenty-Fourth Symposium (International) on Combustion*, The Combustion Institute, Pittsburgh, 1992, pp. 889-898.
12. Miller, J. A. and Bowman, C. T., *Prog. Energy Combust. Sci.* 15:287-338 (1989).
13. Magnussen, B. F., Hjertager, B. H., Olsen, J. G., and Bhaduri, D., *Seventeenth Symposium (International) on Combustion*, The Combustion Institute, Pittsburgh, 1978, pp. 1383-1393.
14. Magnussen, B. F., Nineteenth AIAA Aerospace Meeting, St. Louis, 1981.
15. Magel, H. C., Schneider, R., Risio, B., Schnell, U., and Hein, K. R. G., Eighth International Symposium on Transport Phenomena in Combustion, San Francisco, 1995.
16. Magnussen, B. F., *Eighteenth International Congress on Combustion Engines*, International Council on Combustion Engines, Tianjin, 1989.
17. Gran, I. R., Mathematical Modeling and Numerical Simulation of Chemical Kinetics in Turbulent Combustion, Dr. Ing. Thesis, University of Trondheim, 1994.
18. Glarborg, P., Kee, R. J., Grcar, J. F., and Miller, J. A., "PSR—A Fortran Program for Modeling Well-Stirred Reactors," Sandia National Laboratories Technical report SAND86-8209, 1986.
19. Garreton, D. and Simonin, O., First Aerodynamics of Steady State Combustion Chambers and Furnaces Workshop, EDF-DER, Chaton, 1994.

COMMENTS

C. H. Priddin, Rolls Royce plc., UK. Would you explain why the predicted temperature falls at the end of the reactor? It seems rather sudden.

Author's Reply. The temperature fall after the combustion process is completed is due to the radiative heat loss of this non-adiabatic combustor. The wall temperature of the combustion chamber is only 120°C.

•

Thierry Poinso, IMFT/Cerfacs, France. Did you check the influence of the different model coefficients used for the Eddy Dissipation model?

Author's Reply. We have not yet undertaken any detailed investigation of the influence of all model coefficients. Some variations were made of the flow rate M^* (which defines the residence time inside the fine structure reactor) and of the mass fraction of fine structures γ^* . The major influence was found at the position where ignition occurs, resulting in an axial shift of the calculated profiles.

•

Norberto Fueyo, University of Zaragoza—Litec, Spain. Most CFD models of reburning fail to reproduce the

correct delay of NO formation in the reburning zone, predicting a complete depletion of NO while the experiments show a more moderate delay. Your calculations also exhibit this problem. Do you think this mismatch should be attributed to the chemistry model or to too fast (and too perfect) mixing in the simulation between reburn fuel and primary-combustion gases?

Author's Reply. The question concerns some results which are shown in Magel et al. [1]. These calculations were done using the same model as described in the present paper, but are not included because of space limitations.

In our opinion, it is not a problem of an incorrect predicted mixing between reburn fuel and primary combustion because of the good results in predicting the hydrocarbon chemistry. We think that this mismatch should be attributed to the chemistry model or to the modelling of turbulence-chemistry interaction, i.e. the EDC model. But at present neither hypothesis can be proved.

REFERENCE

1. Magel, H. C., Schnell, U., Hein, K. R. G., *3rd Workshop on Modelling of Chemical Reaction Systems*, Heidelberg, 1996.